geoconvention
Calgary • Canada • May 15-19 2017

Integration of Seismic and Geomechanics for 4D Monitoring - Application to Heavy-oil Reservoir

E. Rebel-Schissele & A. Settari
CGG

Introduction

4D Geomechanics and more specifically integration between seismic and geomechanics is the main topic of this abstract. It deals with the impact of geomechanical changes on reservoir monitoring while producing an oil reservoir. In particular, the influence of geomechanical variations on seismic velocities is shown through stress-sensitive rock physics models.

The analysis considers a heavy-oil reservoir, produced using a well-known process called Steam Assisted Gravity Drainage, or SAGD. In this in-situ, thermal recovery method, two horizontal wells are drilled into the reservoir above each other about 5 meters apart. The upper well injects steam into the reservoir at high pressure and temperature, which is a very effective way to lower the oil viscosity so it can begin to flow via gravity down to the producer. In an ideal homogeneous reservoir, the steam chamber would develop around the well pair as a perfect inverted triangle shape. However, presence of heterogeneities within the reservoir (for example, shale bodies) can slow down or even block the steam chamber progression.

4D seismic is one of the most effective ways to monitor the steam chamber progression. By comparing maps of seismic attributes at different times, the continuous spatial distribution of the heated zones can be approximately located. Such information is the key to optimize the thermal conformance and efficiency of the process and to provide options to successfully adjust the development program (Lopez et al., 2015). 4D seismic refers to the change in travel time and amplitudes that are observed in the analysis of time-lapse surveys. There are several origins for the observed 4D attributes. One origin is directly connected to changes of physical attributes inside the reservoir (pore pressure, temperature, saturations). Another origin occurs both inside and outside the reservoir and is due to stress/strain changes induced by pressure/temperature changes. These stress/strain variations have a double-impact on the 4D attributes. Firstly, they cause expansion/compaction phenomena (changes in reservoir/overburden thicknesses) and secondly, they cause stress-induced changes of the seismic velocities themselves.

In the first part of this abstract, the different steps of the workflow that captures the geomechanical aspects of 4D are briefly presented and in the second part, the methodology has been applied to a synthetic case representative of a typical northern Alberta heavy oil reservoir. Some of the main results are also presented and discussed.

Theory and/or Method

The methodology presented here integrates geomechanical variations in the computation of seismic velocities. It implies the combination of reservoir flow, geomechanics and geophysics. The methodology is applied to a SAGD reservoir, but could be applied to any other type of reservoir where injection/production processes occur. Similar techniques have already been presented (Nauroy, 2013) but very often when the influence of mean effective stress on seismic velocities is studied, only pore pressure variations are considered and the total stresses are assumed constant and set to their values at initial reservoir conditions. As these stresses are varying during the process of steam injection, we propose to compare seismic velocities obtained considering pore pressure variations only with those obtained when both pore pressure and total stresses are varying.

The main steps of the workflow are presented Figure 1. After building a valid numerical model, reservoir and geomechanical simulations are coupled in order to predict the time-evolution of the pressure, temperature, saturations, stresses and strains while injecting high-pressure steam into the reservoir (see

Settari and Walters, 2001 for explanation about GEOSIM, the software used for the coupled simulations presented in this paper). Outputs of the coupled simulation are then taken as inputs to the petro-elastic model (PEM) in order to estimate how much seismic velocities variation should be expected considering that particular SAGD scenario.

The PEM used for the reservoir part is based on granular media theory. The effective stress dependency on dry bulk and shear modulus is taken into account using the Hertz-Mindlin relation by:

$$K_{dry} = K_{dry0}\left(\frac{\sigma'}{\sigma'_0}\right)^{\frac{1}{3}} \quad \text{and} \quad \mu_{dry} = \mu_{dry0}\left(\frac{\sigma'}{\sigma'_0}\right)^{\frac{1}{3}} \qquad (1)$$

where σ' is the average effective stress (differential pressure between the average total stress and the pore-pressure) and the subscript ^{0} indicates initial conditions.

The fluid properties (densities and elastic moduli) depend on temperature and pressure conditions and are updated all along the simulation. At low temperature, the bitumen no longer behaves as liquid (its viscosity is 1.3e6 cP at initial reservoir temperature of 11^oC) and its shear modulus can't be neglected anymore. In addition to temperature, oil viscosity presents a frequency dependency that has not been investigated yet. The FLAG model (Fluids/DHI Consortium) is used to estimate the bulk and shear moduli of the bitumen as a function of temperature and pressure.

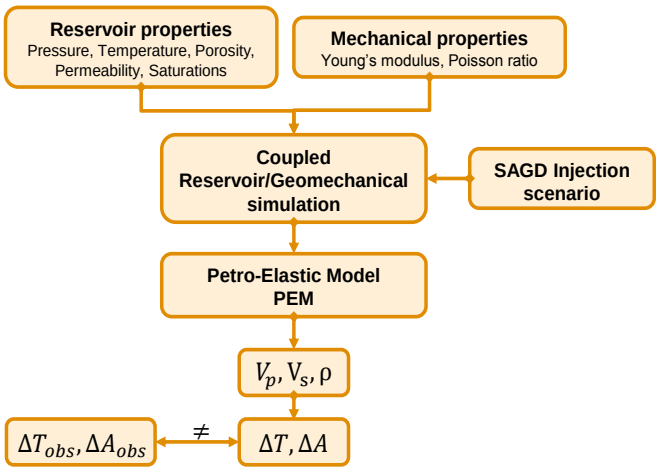

From the dry rock matrix moduli and the fluid properties, the time-evolution of the saturated moduli can be calculated. The highly viscous bitumen doesn't allow us to use the Gassmann equations any longer for fluid substitution and Ciz and Shapiro (2007) approach has been followed instead. The saturated moduli together with the densities are then used to estimate the seismic velocities and the expected 4D attributes (travel time and amplitude variations). If available, these attributes are compared to 4D attributes observed in the field and used to calibrate the coupled reservoir-geomechanical simulations.

Figure 1: General workflow for 4D Geomechanics

Application to a synthetic case – Results and discussion

The workflow described in the previous section has been applied on a synthetic case and the results are given here. The model is based on typical heavy oil reservoirs located in northern Alberta. The depth of the reservoir is 180m and the reservoir itself is 60m thick. The layer thicknesses of each formation as well as the physical attributes describing the reservoir are held constant at initial reservoir conditions, and only a 2D section of the reservoir is considered here (300 meters long). The main parameters used to describe the reservoir (upper and lower McMurray formation, abbreviated McM) are summarized in Table 1. Different ways can be used to couple the reservoir and the geomechanical simulations, and in this case the 2 softwares have been explicitly coupled at each time step, which means that for each time step, the reservoir simulator uses the stresses and strains solution calculated by the geomechanical finite-element code from the previous time step.

	Thickness (m)	Porosity (fraction)	Kh (mD)	Kv (mD)	Sw (fraction)	E (MPa)	Poisson ratio
Upper McM	20	0.35	100	1	0.25	500	0.25
Lower McM	41	0.35	5000	1000	0.15	500	0.25

Table 1: Main parameters used for the coupled reservoir-geomechanical simulation (reservoir part only)

Figure 2 shows the reservoir and geomechanical grid for the Wabisca and McMurray (upper and lower) formations (not represented here are the Clearwater and Devonian formations). The locations of the injector/producer are also represented by 2 crosses and (a), (b), (c) and (d) give the temperature within the reservoir after respectively one, four, eight and twelve years of steam injection.
Figure 3 gives the total stress variations (difference with initial stress states) after twelve years of steam injection. The shape of the horizontal stress variation follows the reservoir temperature shape, with a mean increase of 2.6 MPa between the beginning and the end of injection (Figure 3b). The shape of the vertical stress variation is slightly different (Figure 3a). A smaller increase is observed around the steam chamber (~0.8MPa) and all the way up to the Wabisca formation. A zone of stress decrease (usually due to stress arching effects) is also seen ahead of this zone of increase (blue colour on each side of the steam chamber).

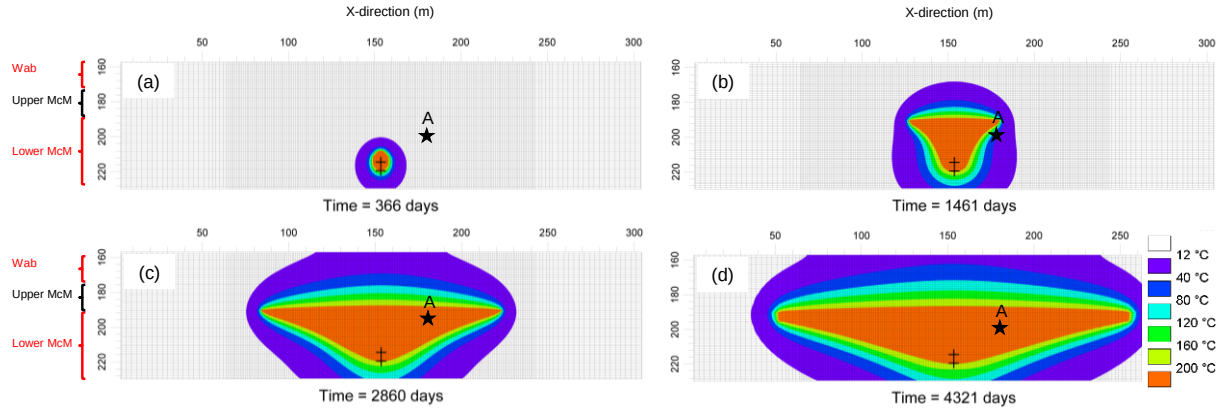

Figure 2: Time-evolution of the temperature within the reservoir after (a) one year, (b) four years, (c) eight years and (d) twelve years of steam injection.

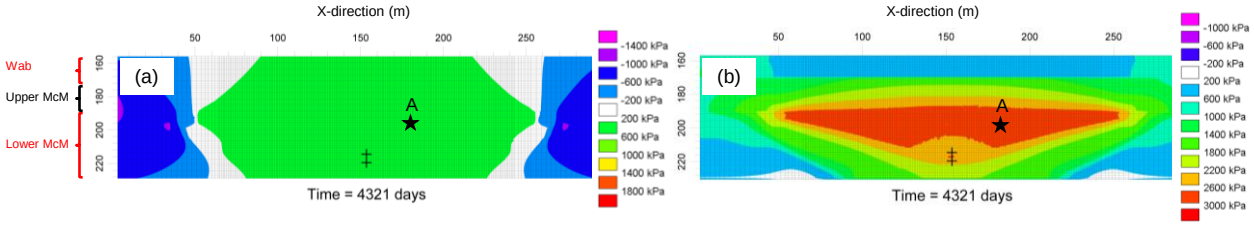

Figure 3: Difference between final and initial stress distribution after twelve years of injection. Panel (a) represents the vertical total stress and panel (b) represents the horizontal total stress.

The analysis of seismic velocities variations with physical attributes within the reservoir is illustrated for a particular point called A (see Figure 2 for its location). **Error! Reference source not found.** represents the time-evolution of the pore-pressure, the temperature, the saturations and the stresses for this particular location. The propagation of different fronts is observed: the pressure front precedes the temperature front, followed by the steam saturation front. As the temperature front propagates into the reservoir, the water saturation increases and the oil saturation decreases. As soon as the steam front arrives, the gas saturation increases. The two last curves represented in **Error! Reference source not found.**e show the evolution of effective stress as a function of time when the variability of mean total stress is taken into account or not. After twelve years of injection, these 2 quantities exhibit a differential of 1.4 MPa.

All the physical attributes represented in **Error! Reference source not found.** have an impact on the seismic velocities. We used these attributes together with our calibrated petro-elastic model to estimate the time-evolution of the seismic velocities and the results are represented **Error! Reference source not found.** for both P and S-waves. These curves allow estimating the individual influence of each physical attribute. For example, the blue curves give the influence of the pore pressure alone while the red curves

give the influence of pore-pressure and temperature together. We observe that the blue and red curves separate as soon as the temperature increases at point A (after 1200 days).

Both temperature and pore-pressure induce a decrease on P- and S-wave velocities while the change in saturation (increase in gas saturation) induces a decrease on P-wave velocity and an increase on S-wave velocity. Comparing the yellow and black dashed curves gives the impact of taking into account the total stress variation in our model. The main effect of not taking into account the total stress variations is to overestimate the seismic velocities changes induced by high-pressure steam injection. While the P-wave ratio between final and initial values at point A was around 40% when considering only changes in pore-pressure, temperature and saturations, it reduces to 28% when total stress variations are additionally taken into account. For the S-wave velocity, this ratio decreases from 22% to 6%. Note that the S-wave velocity curve (black dashed line) reaches a minimum around 1500 days, due to the start of increase in temperature. This feature is important for discriminating the heated zones from the cold ones.

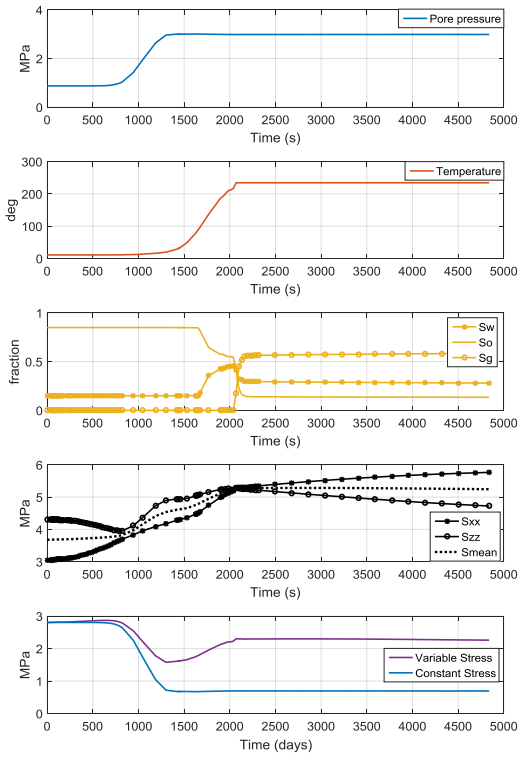

Figure 4: Time-evolution of (a) the pore pressure, (b) the temperature, (c) the saturations, (d) the total stresses and (e) the effective stresses at point A (see Figure 2 for location of point A in the reservoir).

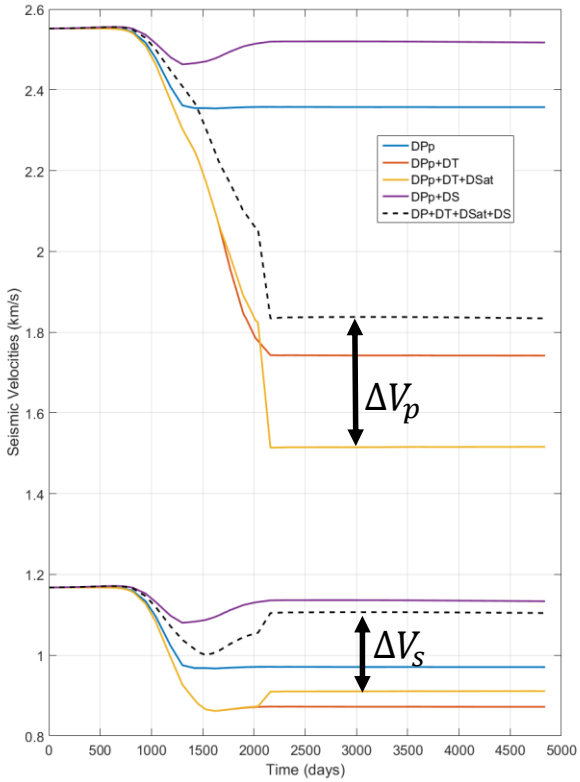

Figure 5: Influence of the different physical attributes (pore pressure, temperature, saturations and stresses) on the P- and S-wave velocities.

Conclusions

In this abstract, the influence of including mean total stress variation in seismic velocities estimation while interpreting 4D attributes variations measured from seismic time-lapse has been shown. Taking into account the mean total stress has a strong impact on seismic velocities and reduces the expected difference of both P- and S-wave velocities between the beginning and the end of steam injection.

Further work is ongoing to account for all three components of the stress field, independently. As vertical and horizontal stresses don't evolve similarly, stress-induced anisotropy has to be expected in the reservoir and in addition to the already anisotropic caprock. Impact of stress variation around more complex structures like reservoir discontinuities (faults) or caprock failure is also being analysed in terms of velocity changes in order to help understanding complex 4D attributes observed on seismic data.

References

Ciz R., Shapiro S.A., 2007, Generalization of Gassmann equations for porous media saturated with a solid material, Geophysics 72, A75-A79.

Lopez, J. L., Wills, P. B., La Follett, J. R., Barker, T. B., Xue, Y., Przybysz-Jarnut, J. K., Potters, J. H. H. M., van Lokven, M., Brouwer, D. R., Berron, C., 2015, Real-Time Seismic Surveillance of Thermal EOR at Peace River, SPE journal, SPE-174459-MS.

Nauroy, J-F., Doan, D.H. Guy, N., Baroni, A., Delage, P., Mainguy, M., 2012, Evolution of seismic velocities in heavy oil sand reservoirs during thermal recovery process, Oil & Gas Science and Technology – Revue d'IFP Energies nouvelles, Institut Francais du Petrole, 67 (6), pp. 1029-1039.

Settari, A. and Walters, D., 2001. Advances in coupled geomechanical and reservoir modeling with applications to reservoir compaction, SPE journal, SPE 51927.